

---

# 14B.1 SST Diurnal Variability and Its Influence on the Tropical Atmospheric Intraseasonal Variability

JIAN LI \*

*Department of Atmospheric, Oceanic and Earth Sciences, George Mason University, Fairfax, Virginia*

BOHUA HUANG

*Department of Atmospheric, Oceanic and Earth Sciences, George Mason University, Fairfax, Virginia*

*Center for Ocean-Land-Atmosphere Studies, Institute of Global Environment and Society, Calverton, Maryland*

## 1. Introduction

The diurnal cycle of sea surface temperature (SST) is a fundamental phenomenon in the world oceans. Early observations of the diurnal variation of SST can be retrieved back to 1940s. For instance, Sverdrup et al. (1942) found that the diurnal SST amplitude is about  $0.2 \sim 0.6^\circ\text{C}$  from in situ measurements of water temperature of upper 1 meter. With the development of remote sensing technique, we are able to measure water temperature within the oceans skin layer of a few millimeters, which reports more dramatic day-night SST differences up to  $2 \sim 3^\circ\text{C}$ , at certain conditions, reaching  $5^\circ\text{C}$  in extreme case.

Partly due to its substantial magnitude, the diurnal SST variation can have impact on lower frequency variability of the climate system. Li et al. (2001) shows the diurnal SST variability can affect the atmosphere over the western Pacific warm pool through reducing the amplitude of latent heat flux on intraseasonal time scale. The air-sea interaction on diurnal time scale may also play an important role in the Madden-Julian Oscillation (MJO) and in turn the El Niño and Southern Oscillation (ENSO), as well as the mean climate (Slingo et al. 2003; Dai and Trenberth 2004).

The SST diurnal variation is fundamentally caused by the large variation in day/night solar radiation reaching the sea surface. Its amplitude and phase, however, depend critically upon the surface wind condition, as well as the oceanic stratification near the sea surface. A few hours after sunrise, a shallow warm layer is formed at the sea surface and quickly reaches its critical depth where the absorbed solar radiation balances the surface heat loss. Afterwards, growing solar heating tends to inhibit its further deepening while the trapped heat increases its

temperature. The further deepening of this diurnal mixed layer is associated with the wind-induced inertial oceanic currents within the layer.

At the bottom of the heated water, its vertical gradient causes the Kelvin-Helmholtz instability when the bulk Richardson number, i.e., the ratio of the stratification to the shear of the diurnal jet, drops below a critical value. The resultant turbulence breaks up the layer interface and speed up entrainment. As the work of the shear stress is used to lift and agitate dense waters from below, the diurnal mixed layer deepens while its temperature cools down. The bulk Richardson number is restored to its neutral or marginally stable value. The surface heating and inertial currents then build up for the next stage of the mixing. This progressive deepening of the mixed layer limits the surface warming phase to only about half of the period while the net heat flux is into the ocean. The depth of the diurnal mixed layer is usually in the range of a few meters.

Current CGCMs generally do not resolve the physical processes described above because of the coarse vertical resolution and inadequate coupling frequency. As a result, the diurnal SST variability is often totally missing or underestimated in CGCM simulations. The effects of air-sea interaction on the diurnal time scale have not been adequately examined. Given the current computational constraints, a more efficient way to simulate SST diurnal variability in CGCMs is to parameterize the effects of the diurnal mixed layer, based on its essential physics. In this study, we have implemented two physical parameterizations of the diurnal mixed layer to a state-of-the-art CGCM. Both parameterization schemes have been proposed by previous studies but yet to be applied to CGCMs, We have fully tested these parameterizations and conducted multi-year simulations and sensitivity experiments with and without the parameterized diurnal mixed layers. With the assistance of parameterizations, we can simulate the SST diurnal variability realistically and investigate its potential influences on the low frequency atmospheric variability, especially on

---

\*Corresponding author address: Jian Li, Department of Atmospheric, Oceanic and Earth Sciences, George Mason University, MSN 6A2, 4400 University Drive Fairfax, VA 22030.  
E-mail: jli9@gmu.edu

the intraseasonal variability over tropical Indo-Pacific region. The model and experiment design is described in the next section. The results are shown in Section 3. The summary and conclusion are given in Section 4.

## 2. Model and Experiments

We have used the Climate Forecast System (CFS) developed at the National Centers for Environmental Prediction (NCEP). CFS is a fully coupled climate system representing the interaction between the Earth's oceans, land and atmosphere. Currently the CFS is being used for the operational climate prediction at NCEP. The atmospheric component of the CFS is a spectral model of atmospheric primitive equations with a triangular truncation at wave number 62 (equivalent to nearly a 200km Gaussian grid) horizontally and 64 sigma levels from earth's surface to the top of the atmosphere (about 0.27hPa) vertically. Its oceanic component is the Modular Ocean Model version 3 (MOM3) developed by the Geophysical Fluid Dynamics Laboratory(GFDL). The model domain encompasses non-polar world oceans within 74°S and 64°N with zonal resolution as 1°, while the meridional resolution is 1/3° between 10°S and 10°N, gradually increasing through Tropics until becoming fixed at 1° poleward of 30°S and 30°N. It has 40 vertical levels in height coordinate, with a 10-m resolution from the sea surface to 240m depth and 27 levels in the upper 400m, the bottom depth is around 4.5km.

The operational CFS was designed for daily coupling, which exchange daily averaged surface momentum, heat, and freshwater fluxes and SST between two components once a day. Such coupling interval, however, totally suppressed the diurnal SST variability in the model. Our first experiment (control run, CTL hereafter) is to increase the coupling frequency to every three hours and to exchange 3-hourly averaged flux/SST between the two components. The CTL simulation is carried out for 20 years. This simulation allows the diurnal adjustment of the surface fluxes into the ocean. However, increasing the coupling frequency alone is inadequate to resolve the near-surface diurnal mixing processes. Our test also shows the diurnal SST change in CTL is negligible in most of the places. To improve the simulation of the diurnal SST variability, two parameterizations of the diurnal mixed layer by Zeng and Beljaars (2005), (ZB hereafter) and Schiller and Godfrey (2005)(SG hereafter) have been implemented on CFS.

The ZB parameterization assumes that a layer of strong diurnal cycle is embedded within the first vertical grid of an ocean model. At the top of this ocean layer, they also consider a thin skin layer with depth about several millimeters, where molecular heat transport becomes dominant and the heat loss at the surface leads to a cold skin. It is further assumed that the embedded (skin plus diurnal) sub-layer occupies the upper 3 meters of the model grid, at the bot-

tom of which the temperature is the same as the mean temperature of the grid predicted by the ocean model. The temperature change within the sub-layer is parameterized with a prescribed vertical profile. The skin temperature is predicted by the net heat flux at the sea surface and the turbulent heat transport within and at the bottom of the sub-layer.

The SG parameterization also considers an embedded sub-layer of warm water in the upper portion of the top grid of an ocean model. This sub-layer is transient because it exists on when the total heat flux received by the model grid is positive. The depth of the sub-layer changes dynamically to maintain the balance of the turbulent kinetic energy between the surface heat flux and wind-induced entrainment at the bottom. Temperature is assumed to be constant within the sub-layer and the weighted mean of the sub-layer temperature and the temperatures of the rest of the waters in the grid equals to the model-predicted grid temperature. During the day-time, the predicted sub-layer temperature is used as the SST.

After extensive testing, CFS simulations are also performed 20-year integrations with two diurnal mixed layer parameterizations respectively. The simulated SST diurnal variability and its influence on tropical intraseasonal variability will be discussed in the following section.

## 3. Results

### a. SST Diurnal Variability

The model simulated diurnal SST variability is compared with the in situ SST observations from the TOGA TAO/TRITON moorings in tropical region. To extract the intermittent diurnal SST signals with variable amplitude from the total field, a novel data analysis method, the Ensemble Empirical Mode Decomposition (EEMD, Wu and Huang 2009), has been applied. EEMD is a noise-assisted algorithm to separate signals of different time scales adaptive to local frequencies. Its efficiency to decompose multi-scaled time series into limited number of components has been demonstrated by previous studies.

As an example, the TOGA TAO/TRITON SST observed in year 2009 at site 0°N 147°E is shown in Fig.1a and its diurnal component extracted by EEMD in Fig.1b. At this location, a significant diurnal signal is superimposed on the slower variations. The magnitude of the diurnal cycle can reach one degree, which is comparable with the amplitude of seasonal variability. The strongest diurnal signal accompanies the SST warming trend while SST cooling primarily leads to the suppressed diurnal cycle. Such intermittent feature of the amplitude of SST diurnal variability reflects the influences of local meteorological conditions, which also implies a certain degree of interdependence of the SST variability on different time scales.

The simulated and observed SST diurnal signals are

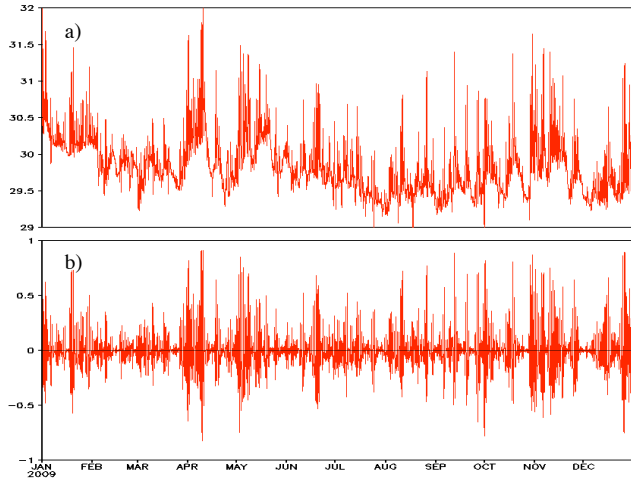


FIG. 1. TOGA/TRITON observed hourly SST at  $147^{\circ}\text{E}$ , Equator in year 2009. a) original SST time series b) diurnal mode extracted with EEMD

compared in Fig.2, together with the surface wind speed and incoming solar radiative flux. The time series of the variables from different runs were taken at the model grid point near  $0^{\circ}\text{N}$   $147^{\circ}\text{E}$ . A 30-day segment is chosen for each run. In general, the amplitude of the SST diurnal variability is unrealistically small in the CTL run (Fig.2d), in comparison with the observations (Fig.2a). The implementations of both mixed layer parameterizations lead significant improvements on the SST diurnal cycle. Especially, the ZB scheme is more effective and produces the strength of diurnal cycle comparable with the observations, as well as the correct phase relation with the incoming solar radiation. In the runs with parameterized diurnal layers, the model also correctly responded to the surface wind variation, with stronger wind suppressing the SST diurnal variability, as confirmed by the observation. Similar comparisons were performed at other buoy sites, and the results suggested that the mixed layer parameterizations were capable of producing realistic SST diurnal variability.

We have further investigated the temporal-spatial distribution of the amplitude of the CFS simulated SST diurnal cycle throughout the tropical area. The amplitude of diurnal SST variation (DSST) is defined as the difference between its daytime maximum and the nighttime minimum at each ocean grid point. Mean DSST fields, averaged over the entire 20-year for each run, show that the regions with substantial SST diurnal variability from the simulations are comparable to the observations. In particular, the northern Indian Ocean, the equatorial western and eastern Pacific, as well as many coastal regions, such as those at the western Central America and West Africa, all show high

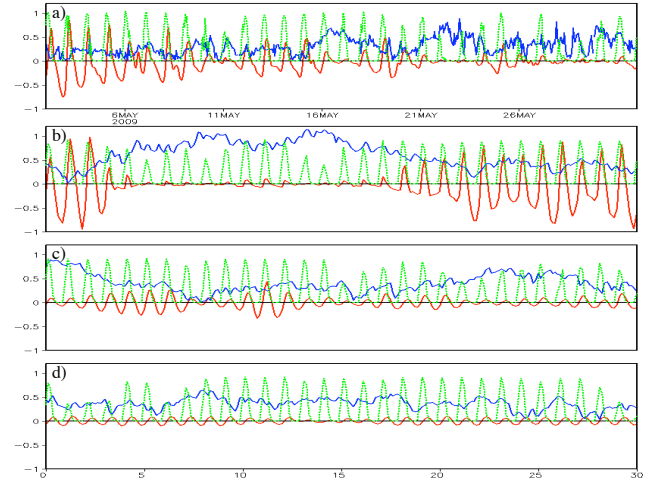


FIG. 2. Diurnal modes of SST variability (red solid) extracted from a) TOGA/TRITON observation at  $147^{\circ}\text{E}$ , Equator, b) ZB experiment at grid point near the observation, c) SG experiment, and d) CTL experiment. Corresponding net solar radiation (green dot, unit:  $10^3 \text{ W m}^{-2}$ ) and surface wind speed (blue solid, unit:  $10 \text{ m s}^{-1}$ ) were shown.

DSST, with values above  $1.0^{\circ}\text{C}$  in the ZB run and  $0.5^{\circ}\text{C}$  in the SG scheme. Most variations of DSST are explained by the wind speed variability across the basin, although lower value of short wave radiation along the convection zone also contributes to the smaller SST diurnal variability. Higher mean DSSTs are generally located in areas where the mean 10-meter wind speed were around  $3\sim 4 \text{ m s}^{-1}$  or below. (Figures not shown). Such spatial distribution of diurnal SST variability is highly comparable with the reconstructed DSST dataset based on observed meteorological variables (Clayson and Weitlich 2007).

To further explore spatial patterns and seasonality of DSST, EOF analyses of the DSST field from the ZB experiment were performed for the Indian, Pacific and Atlantic Oceans respectively. The three leading EOF modes for Indian Ocean basin are shown in Fig.3. The spatial pattern of the first mode (Fig.3a) indicates that the DSSTs have the same sign across the basin. Its time series (Fig.3b) shows that the strongest day-time warming occurs around March and April while the DSST values are at the minimum from May to August. This variability is due to the effect of the summer monsoon, as the monsoon brings convective rainfall and strong surface wind over most of the ocean basin. The second mode (Fig.3c) features a general asymmetry between the northern and southern hemispheres. Its time series (Fig.3d) is characterized with both annual and semi-annual components, showing that the DSST in the north-

ern ocean is at its minimum (maximum) during boreal winter (spring) while a pair of secondary peak and valley appears in boreal summer and fall. The seasonal contrast of the incoming solar radiation primarily determines the spatial distribution of DSST. Meanwhile Indian monsoon may also play secondary role in modulating the amplitude of DSST semi-annually, especially during boreal summer. The third mode (Fig.3e) shows an east-west ocean dipole with the DSST is enhanced in the eastern equatorial Indian Ocean near the Sumatra while weakened around the African coast. Its time series also bear a semi-annual signature, with larger DSST near the Sumatra coast during boreal spring and fall (Fig.3f). On top of the semi-annual signals, the time series also shows significant year-to-year fluctuations. This spatial pattern is also reminiscent of the leading SST interannual variability at the equatorial Indian Ocean, the so-called Indian Ocean dipole. (IOD, Saji et al. 1999).

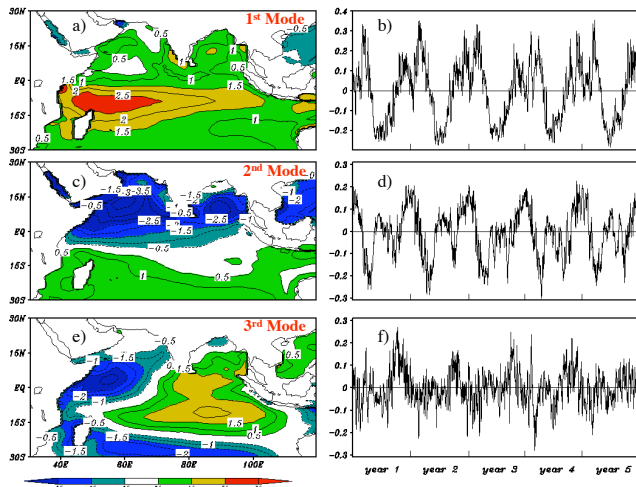


FIG. 3. Leading EOFs spatial patterns (left, a), c), e), ) and principle components (right, b), d), f) ) of the amplitude of diurnal SST variability (DSST) in Indian Ocean basin.

In other two basins, the variations of daytime warming amplitude are also dominated by the seasonal cycle (Figures not shown). For instance, the east-west dipole also appears in the Pacific (EOF 2) and Atlantic (EOF 3). The Atlantic DSST dipole indicates the influence of the West African monsoon. The dipole in the Pacific Ocean might reflect the pattern of ENSO.

*b. Influence of diurnal SST variations on the intraseasonal variability*

In this section, we examine the potential effects of the enhanced diurnal SST variability on the tropical intraseasonal

variability, or the Madden-Julian Oscillation (MJO). We have used the MJO index defined by Wheeler and Hendon (2004) to characterize the phases of the model simulated MJO, which is based on the principal components of the two leading multivariate EOF analysis of the equatorial-averaged ( $15^{\circ}\text{S}$ - $15^{\circ}\text{N}$ ) anomalies of OLR and zonal wind at 850hPa and 200hPa. We have used the MJO index to generate the composite MJO life cycle for both the CTL and ZB experiments, respectively. For both multivariate EOF and composite analyses, unfiltered anomalies are computed by subtracting the climatological daily mean calculated over all years of data. Intraseasonal (20-100 day) bandpass-filtered anomalies are then constructed using a 201-point Lanczos filter, which has half-power points at 20- and 100-day periods.

Both simulations have generated realistic MJO, with dominant periods somewhat lower than the observations, based on the the EOFs derived from NOAA OLR, and NCEP1 850- and 200-hPa zonal wind. A power spectrum analysis of the leading principle components of CTL and ZB does not show a significant difference between the dominant periods of the intraseasonal variability simulated by the two experiments. Several critical features of the observed MJO have been well reproduced by both simulations, including the out-of-phase relationship between lower- and upper-tropospheric wind anomalies, and the strong lower-tropospheric westerly anomalies near the west of enhanced convection. However, the MJOs in both runs explain relatively small amounts of total variance, in comparison with the observations. Between the two runs, the ZB shows larger amplitude of wind anomalies for upper- and lower-troposphere than that of CTL. Meanwhile, the location of convection is shifted eastward in ZB experiment comparing with CTL which makes the phase relationship between equatorial convection and zonal wind anomalies in ZB experiment much comparable to that of observation.

We have conducted composite MJO life cycle, which is divided into eight phases based on the MJO index. For each phase, composites are generated by averaging over all days that exceed a specified amplitude threshold of the MJO index. The composite fields are generated for precipitation, amplitude of diurnal SST variability (DSST), SST and 850hPa zonal wind in the Indo-Pacific region for both boreal summer and winter seasons respectively. Both the ZB and CTL experiments exhibit realistic propagation features of convection, such as the eastward movement during boreal winter and northeastward propagation in Indian Ocean during boreal summer. The phase relationship between spatial structures of precipitation and zonal wind anomaly is consistent with observation.

The most dramatic difference between ZB and CTL experiments is the modulation of the DSST during the different phases of the MJO life cycle. The DSST anomalies propagate northward and eastward during boreal sum-

mer (mainly eastward during boreal winter) following the movement of the convection correspondingly. The negative(positive) DSST anomalies lag the positive(negative) precipitation anomalies for 3 to 5 days which indicates the modulation of DSST anomalies by the active(suppressed) phase of MJO. Meanwhile, SST anomalies in ZB also show significant change from CTL on each phase of MJO life cycle. Particularly during boreal summer, the amplitude and spatial extension of SST anomalies in Indian Ocean basin and near maritime continent are significantly enhanced almost in every phase of life cycle (as in Fig.4). We also noted that the DSST has coherent spatial pattern with SST anomalies and slightly leading the SST variation. Therefore, it is likely to contribute a portion of intensified SST anomalies. In the boreal winter composite, such enhancement also occurs in several but not all phases.

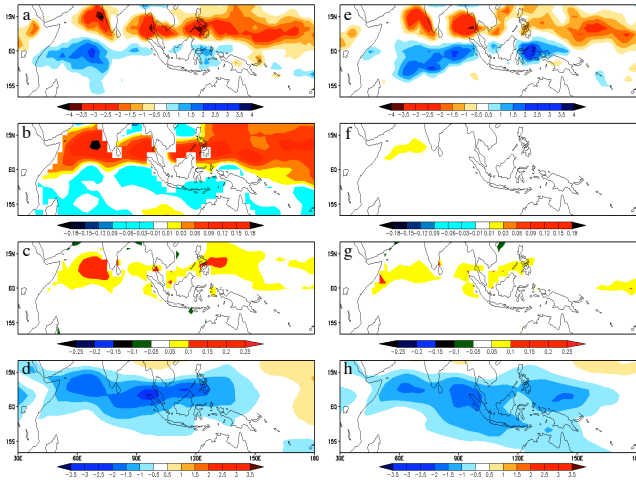


FIG. 4. One of eight phases of MJO life cycle composite during boreal summer (May-Oct.) on surface precipitation (a, e), amplitude of diurnal SST variability(b,f), sea surface temperature(c,g) and 850hPa zonal wind(e,h)for ZB (a-d) and CTL (e-h) experiments, respectively

To understand the variation of SST anomalies in ZB experiment, we performed a lag-longitude diagnosis of SST anomalies against 850hPa velocity potential anomalies for both the CTL and ZB runs (Fig.5). The anomalies of 850hPa velocity potential was averaged across 60~70°E and 5°S~5°N, which characterizes the convection in this region. The lag correlation of SST was average between 15°S~15°N. The results show a different relation between the convection and SST in the ZB run than in the CTL run. First, the largest SST response is shifted further to the east of the convection in the ZB while the largest SST response is at the same location as the convection in the CTL run. Second, the lag of the SST response is shortened

in the ZB run where the large negative correlation coefficient (-0.4) starts at zero lag-day, which suggests that the SST warming (cooling) occurs almost simultaneously with divergence (convergence) of lower troposphere. The corresponding change in the CTL run, however, shows a longer delay of a few days. We speculate that this is mostly because the enhanced diurnal SST variability during the divergence period speeds up the warming of the sea surface during this phase.

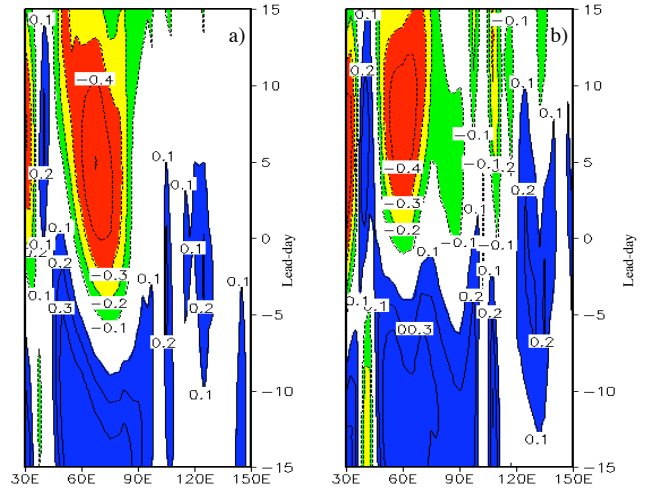


FIG. 5. Lead-lag correlation between 850hPa velocity potential anomaly and equatorial SST anomaly for ZB (a) and CTL (b) experiments. Velocity potential has been averaged over 60~70°E and 5°S~5°N in Indian Ocean. Positive lead-day indicates velocity potential leading SST

#### 4. Summary

The SST diurnal variability and its influence on weather and climate have attracted increasing attentions during recent years. Yet most current CGCMs fail to simulate the amplitude of the SST diurnal variability for the lack of capability of resolving the diurnal mixed layer near the sea surface. The purpose of this research is to simulate SST diurnal variability in NCEP Climate Forecast System through the parameterization of the diurnal mixed layer and to examine the possible effects of the diurnal SST variability on the lower frequency weather and climate variability such as the Madden-Julian Oscillation

Our model experiments using CFS show that SST diurnal cycle, as well as its temporal intermittence, can be simulated realistically in current CGCMs with parameterized diurnal mixed layer. The diurnal mixed layer parameterization is economical and effective approach to reproduce SST diurnal variability realistically in CGCMs at a relatively low computational cost.

Our results also show that the amplitude of SST diurnal cycle depends on the local weather conditions. The large daytime warming mainly happens when the wind is light and net solar radiation is large. Both mixed layer parameterizations are sensitive to the atmospheric variation and are able to reflect the weather influence on SST diurnal cycle. With these parameterizations, the intermittent and sporadic nature of the SST diurnal variability can be fully simulated in CGCMs, which is compared favorably with the in situ observations. Moreover, large-scale distributions of the diurnal SST amplitudes, as well as its seasonal variability, can also be realistically produced.

Our further examination shows that the modulation of the SST diurnal cycle is an integral part of the MJO and may have some influence on the intraseasonal ocean-atmosphere oscillation. The amplitude of the SST diurnal cycle is generally enhanced during the suppressed MJO phases in the Indian Ocean, and speed up the warming of the sea surface during this period. The SST anomalies in Indian ocean has significant increasing when the SST diurnal variability is adequately simulated in the CGCM.

## REFERENCES

- Clayson, C. and D. Weitlich, 2007: Variability of tropical diurnal sea surface temperature. *J. Climate*, **20**, 334–352.
- Dai, A. and K. E. Trenberth, 2004: The diurnal cycle and its depiction in the community climate system model. *J. Climate*, **17**, 930–951.
- Li, W., R. Yu, H. Liu, and Y. Yu, 2001: Impacts of diurnal cycle of sst on the interseasonal variation of surface heat flux over the western pacific warm pool. *Adv. Atmos. Sci.*, **18**, 793–806.
- Saji, N. H., B. N. Goswami, P. N. Vinayachandran, and T. Yamagata, 1999: A dipole mode in the tropical indian ocean. *Nature*, **401**, 360–363.
- Schiller, A. and J. S. Godfrey, 2005: A diagnostic model of the diurnal cycle of sea surface temperature for use in coupled ocean-atmosphere models. *J. Geophys. Res.*, **110**, C11 014, doi:10.1029/2005JC002975.
- Slingo, J. M., P. Inness, R. Neale, S. Woolnough, and G. Y. Yang, 2003: Scale interactions on diurnal to seasonal timescales and their relevance to model systematic errors. *Ann. Geophys.*, **46**, 139–155.
- Sverdrup, H. U., M. W. Johnson, and R. H. Fleming, 1942: *The oceans : Their Physics, Chemistry and General Biology*. Prentice-Hall, Englewood Cliffs, New York, 1087 pp.
- Wheeler, M. C. and H. H. Hendon, 2004: An all-season real-time multivariate mjo index: Development of an index for monitoring and prediction. *Mon. Wea. Rev.*, **132**, 1917–1932.
- Wu, Z. and N. E. Huang, 2009: Ensemble empirical mode decomposition: a noise-assisted data analysis method. *Advances in Adaptive data Analysis*, **1**, 177–229.
- Zeng, X. and A. Beljaars, 2005: A prognostic scheme of sea surface skin temperature for modeling and data assimilation. *Geophys. Res. Lett.*, **25**, 1411–1414.